

Gravitational Lensing by Cosmic String Loops

Andrew A de Laix and Tanmay Vachaspati

Case Western Reserve University

Department of physics

Cleveland, OH 44106-7079

(October 11, 2018)

We calculate the deflection of a light ray caused by the gravitational field of a cosmic string loop in the weak field limit and reduce the problem to a single quadrature over a time slice of the loop's world sheet. We then apply this formalism to the problem of gravitational lensing by cosmic string loops. In particular, we find an analytic solution for the special case of a circular loop perpendicular to the optical axis. As examples of more complicated loops, we consider two loops with higher frequency Fourier modes. The numerical analysis illustrates the general features of loop lenses. Our estimates, using typical parameters for GUT scale loops, show that the stringy nature of loop lenses can be observed for lensing systems involving high redshift galaxies ($z \sim 2$), and we suggest that gravitational lensing can confirm the existence of GUT scale strings if they are the seeds for large scale structure formation.

11.27, 98.80.C, 95.30.S, 98.62.S

I. INTRODUCTION

Current research focuses on two scenarios for the formation of structure in the universe: the first where structure formation was seeded by adiabatic perturbations produced during an inflationary epoch and the second where structure accretes around isocurvature perturbations produced by topological defects such as cosmic strings, global monopoles or textures. In the latter scenario it should be possible to directly detect the presence of topological defects in the present universe leading to immediate confirmation of the scenario. On the other hand, the lack of direct evidence for topological defects in the present universe can lead to constraints on the defect scenario for structure formation and perhaps be considered as circumstantial evidence in favor of the inflationary alternative. Thus it is quite important to consider specific distinctive signatures of the various topological defects that can be used to directly observe them.

Let us specifically consider cosmic strings, the model which will be relevant to the work in this paper (for a review of cosmic strings, see Ref. [1]). A number of observable features produced by cosmic strings of mass density suitable for structure formation have been discussed in the literature. These include discontinuous patterns in the microwave background radiation [2], generation of a gravitational wave background that could be detected by noise in the millisecond pulsar timing [3] and gravitational lensing [4,5,6,7,8]. The ongoing observations of anisotropies in the microwave background radiation are expected to yield stronger constraints or positive results over the next decade or so. The millisecond pulsar observations can only impose tighter constraints on the string scenario since a positive detection of gravitational waves does not specifically imply the existence of cosmic strings. There has also been sporadic effort over the last decade to work out the gravitational lensing signature of cosmic strings but, perhaps due to the difficulties encountered in understanding the evolution of the string network, no distinctive result emerged from these analyses. However, an analytical framework for describing the string network has been constructed over the last few years and the time seems ripe to reconsider gravitational lensing as a tool for searching for strings. The timing is also right from the observational viewpoint since several new initiatives are underway that promise to survey much wider and deeper regions of the sky.

In this paper we investigate gravitational lensing by cosmic string loops¹. We begin in Sec. II by estimating the probability of string lensing and in so doing we review some of the relevant properties of cosmic strings. Our estimates are based on recent results for the string network evolution summarized in Ref. [1]. Next, in Sec. III, we consider photon propagation in the metric of a loop. The problem appears to be quite difficult at first because the oscillating loop is a complicated time dependent gravitational source. Yet we are able to show that the problem reduces to one that is static where a specific time slice of the loop's world sheet is sufficient to determine the gravitational lensing

¹Gravitational lensing by global monopoles and textures is likely to be less interesting since only a few of these are expected to occur within our horizon. Also, their spherical symmetry will lead to lensing that is harder to differentiate from that due to conventional sources.

effects. In other words, the bending of light by a string loop is equivalent to the bending of light by a static curved rod with non-uniform energy density, a result similar to that for the energy shift of a photon propagating in a string loop background first derived by Stebbins [9]. We also rederive the energy shift of the photon in the Appendix and recover a logarithmic term that appears to have been eliminated by the regularization procedure used in Ref. [9].

Once we have set up the formalism for an arbitrary loop and described some rudiments of gravitational lensing theory (Sec. IV A), we apply it to treat the lensing due to a circular loop that is oriented in a plane normal to the optical axis (Sec. IV B). The results for the circular loop are in agreement with the assumption in Ref. [5] that the photons passing through the loop remain undeflected. The deflection of a photon trajectory not threading the loop can also be described quite simply and the whole problem can happily be solved by hand without resorting to numerical evaluation.

The perpendicular circular loop, however, is a very special case as even a change in the orientation of the loop yields qualitatively different results, and loops with less symmetry have completely different lensing behavior. The assumption that photons passing through the loop remain undeflected fails for general loops. We study the lensing due to several generic loops numerically and provide image maps that promise to distinguish cosmic string lensed images from more conventional gravitational lensing events (Sec. IV C). Here we also show that the Einstein radius of the string loop is comparable to the typical loop size for any value of the string tension and so the stringy nature of the loop plays a crucial role in determining the structure of the lensed images. Effective techniques — for example, techniques that replace the string loop by a point mass plus perturbations — are unlikely to yield successful approximations leading us to conclude that string loop lenses ought to be observationally distinct from garden variety astrophysical lenses.

In Sec. V we summarize and discuss our main results. We also qualitatively discuss the effects of long strings and describe further work to come. Finally, Sec. VI contains some concluding remarks.

II. LENSING PROBABILITIES WITH STRING LOOPS

Gravitational lensing by cosmic string loops is an interesting problem only if there is a realistic chance of observing a loop lens. In this section, we will estimate the typical size and number density of loops and use these values to determine the likelihood of observing a string loop. Our arguments will be based on scaling solutions to the string network evolution which are indicated by numerical simulations and semi-analytic treatments (for a review of scaling solutions see Ref. [1]).

The string network consists of two components — the long (or infinite) strings and the closed string loops — assumed to have formed during a phase transition in the very early universe. If the strings are to seed large-scale structure formation, they should have a linear mass density $\mu \sim 10^{22}$ gms/cm (conveniently expressed in Planck units as $G\mu \sim 2 \times 10^{-6}$ where G is Newton's gravitational constant). At any epoch in the history of the universe, curved sections of strings will oscillate under their own force of tension; colliding and intersecting strings will undergo reconnections; the strings will stretch under the influence of the Hubble expansion, and the oscillating strings will lose energy primarily to gravitational radiation. The complicated evolution of the string network has been studied in a number of works and a consensus is emerging that the long strings obey a scaling solution [10,11]. In other words, the energy density in the long strings scales with time as $\rho_L \sim 1/t^2$ and the typical distance between strings also scales with time, $L \propto t$, where there are on the order of 10 long strings per horizon at any epoch. The reconnections of long strings and large loops are found to copiously produce small loops. But there is generally less agreement on the precise number density of loops present at any epoch. If the typical loop produced is assumed to have a length $\ell \sim \alpha t$, then numerical results (that do not take the gravitational back reaction into account) place an upper limit of $\alpha < 10^{-3}$ [10,11]. To get a lower limit on α , one supposes that highly curved sections of string straighten out on very short time scales due to gravitational radiation which occurs at a rate

$$\frac{dE}{dt} = \Gamma G\mu^2 \quad (1)$$

where, Γ is a numerical factor depending on the shape of the loop and has been evaluated to be ~ 60 by considering several classes of loops. Since the size of the loops is related to the curvature of strings, the smallest loops that can be produced are those that have lifetimes longer than the Hubble time scale. This leads to $\alpha \approx \Gamma G\mu \sim 10^{-4}$ which we will use for the purpose of numerical estimates. Then, for a scaling solution, the number density of loops with length between ℓ and $\ell + d\ell$ at a given time t is

$$dn(\ell, t) \approx \frac{v d\ell}{t^2(\ell + \Gamma G\mu t)^2}, \quad (2)$$

where ν is about 0.5 [1]. Now we can estimate the solid angle of sky coverage necessary to observe a string loop lens. Using eq. (2), the number of loops of length between αt and $\beta\alpha t$ — supposing that loops larger than $\beta\alpha t$ will not make interesting lenses — per solid angle at redshifts less than z_0 is

$$\frac{dN_l}{d\Omega} = \int_0^{z_0} dz \int_{\alpha t}^{\beta\alpha t} d\ell \frac{4}{H_0^3} \frac{dn(\ell, t)}{d\ell} \frac{1}{(1+z)^6} \frac{(1+z - \sqrt{1+z})^2}{\sqrt{1+z}}, \quad (3)$$

where $t = (2/3)H_0^{-1}(1+z)^{-3/2}$. The various explicit factors of the redshift arise from the changing volume element in an expanding universe. One can evaluate this integral analytically and find the result

$$\frac{dN_l}{d\Omega} = \frac{27}{2} \frac{\nu\alpha(\beta-1)}{(\beta\alpha + \Gamma G\mu)(\alpha + \Gamma G\mu)} [\ln(1+z_0) + z_0 - 4\sqrt{1+z_0} + 4]. \quad (4)$$

For $z_0 = 1$, $\beta \sim 2$ and $\alpha = \Gamma G\mu$, there are about 400 $(\Gamma G\mu_4)^{-1}$ loops per steradian which corresponds to about 1 loop for every $(3^\circ)^2 \Gamma G\mu_4$ of sky, where we have defined $\Gamma G\mu_4 = \Gamma G\mu \times 10^4$. But, this does not necessarily tell us how many loop lenses we can expect to observe because we have not yet factored in the odds that a galaxy will be near enough to a given loop to be significantly lensed. To resolve this problem we require the luminosity distribution of high redshift galaxies.

For an order of magnitude estimate of the luminosity distribution of high redshift galaxies, we can use information about nearby galaxies and extrapolate to higher redshifts. Such an extrapolation is justified only if the effects of evolution can be ignored and we shall assume that this is the case. The local luminosity function, ϕ , is reasonably approximated by the Schechter function [12],

$$\phi(u) = \phi_* u^\alpha e^{-u}, \quad (5)$$

where u is proportional to the luminosity, $\alpha = 1.07 \pm .05$, $\phi_* = 0.010 e^{\pm 4} h^3 \text{ Mpc}^{-3}$ and h is the Hubble parameter in units of $100 \text{ km s}^{-1} \text{ Mpc}^{-1}$. The number density of galaxies, N_g , per unit solid angle per unit redshift per unit flux is given by

$$\frac{d^3 N_g}{d\Omega dz d\kappa} = 4\pi H_0^{-5} z^4 \phi(\kappa z^2), \quad (6)$$

where κ is proportional to the flux. For a flux limited or equivalently a magnitude limited survey, we integrate over κ from a lower bound to infinity. The lower bound can be expressed in terms of the apparent magnitude m using the relation

$$\kappa = 9.0 \times 10^{16} h^{-2} 10^{M_* - m}, \quad (7)$$

where $M_* = -19.53 \pm .25 + 5 \log h$ is the absolute magnitude of a characteristic galaxy and a reasonable value for the magnitude limit is $m = 24$. For a flat universe with no cosmological constant, age constraints suggest that we should use a value of $h = 0.5$ which gives a lower bound of $\kappa = 0.057$. We can express the integral over the flux in terms of an incomplete gamma function which gives us

$$\frac{d^2 N_g}{d\Omega dz} = 2.7 \times 10^8 z^2 \Gamma(\alpha + 1, 0.057 z^2). \quad (8)$$

Let us suppose that we have a loop located at about a redshift of one away from us and we are observing galaxies that are about a redshift of two to three. Then integrating eq. (8) tells us that there are about 1.4×10^9 galaxies per steradian to work with. The typical angular separation between galaxies is about 5.6 arc seconds, which we shall see in Sec. IV C is small enough that a foreground string loop can always be expected to have a galaxy in its background. Therefore every loop has a good chance of being seen as a gravitational lens.

III. GEODESIC DEFLECTION BY A STRING LOOP

In this section, we consider the deflection of null geodesics in the presence of a cosmic string loop, which in the limit of geometric optics, will correspond to the photon paths. (Readers only interested in lensing applications might wish to proceed directly to the final result given at the end of the section.) We shall assume that the background space-time is flat Minkowski space, and ignore the effects of curvature or universal expansion. Since we are interested in loops with radii much smaller than the horizon or curvature scale, this approximation will be valid for determining

the photon deflection. We shall further assume that the string contribution to the metric is weak and may be treated as a perturbation on the flat space. Thus we may write the complete metric as

$$g_{\mu\nu} = \eta_{\mu\nu} + h_{\mu\nu}, \quad (9)$$

where we use the convention $\eta = \text{diag}(-1, 1, 1, 1)$, and $h_{\mu\nu}$ is a small perturbation, so all terms of $O(h^2)$ will be ignored. To fix the gauge, we apply the harmonic condition, that is $g^{\mu\nu}\Gamma_{\mu\nu}^\lambda = 0$, which leaves us with a simple wave equation for the metric

$$\square^2 h_{\mu\nu} = -16\pi G S_{\mu\nu}, \quad (10)$$

where $S_{\mu\nu}$ is related to the stress-energy tensor by $S_{\mu\nu} = T_{\mu\nu} - 1/2\eta_{\mu\nu}T^\lambda_\lambda$. It should be noted that for a loop of finite size, the metric far from the loop is asymptotically flat.

In the geometric limit, we can treat the trajectories of photons as the null geodesics of the metric. If λ is an affine parameter, then the momenta are given by

$$P^\mu = \frac{dx^\mu}{d\lambda}. \quad (11)$$

The evolution of the P^α are determined by the geodesic equation

$$\frac{dP^\alpha}{d\lambda} + \Gamma_{\mu\nu}^\alpha P^\mu P^\nu = 0, \quad (12)$$

with the constraint $P^\mu P_\mu = 0$. In the weak field limit, the Christoffel symbol, Γ , is

$$\Gamma_{\mu\nu}^\alpha = \frac{1}{2}\eta^{\alpha\delta}(h_{\mu\delta,\nu} + h_{\nu\delta,\mu} - h_{\mu\nu,\delta}). \quad (13)$$

To zeroth order, *i.e.* in the absence of a loop, the Christoffel symbol vanishes, implying the momenta are constants and the coordinates grow linearly with λ . In particular, one can choose the affine parameter λ to be t/P^0 . Also, since the non-zero Christoffel components are all first order, we can contract Γ with the zeroth order momenta, and further consider the Christoffel components to be functions of only the zeroth order coordinates. Let us be explicit by considering the dimensionless four velocity which is defined by $\gamma^\mu = P^\mu/P_{(0)}^0$ where $P_{(0)}^0$ is the zeroth order energy. It has a zeroth and first order part which we may write as $\gamma^\mu = \gamma_{(0)}^\mu + \gamma_{(1)}^\mu$. Rewriting eq. (12) using the appropriate substitutions, to first order we get

$$\frac{d\gamma_{\alpha(1)}}{dt} = -(h_{\mu\alpha,\nu} - \frac{1}{2}h_{\mu\nu,\alpha})\gamma_{(0)}^\mu\gamma_{(0)}^\nu. \quad (14)$$

Let us now consider the light ray emitted from a static source residing at a distance much greater than the size of the loop and traveling to a distant observer, that is, we will consider our source and observer to lie effectively at infinity where spacetime is flat. The components of γ^μ which appear explicitly on the right hand side of eq. (14) are zeroth order, and the perturbation in the metric $h_{\mu\nu}$ is a function only of the zeroth order coordinates. Therefore, we can integrate eq. (14) explicitly giving

$$\gamma_{\alpha(1)} = -\int_{-\infty}^{\infty} dt (h_{\mu\alpha,\nu} - \frac{1}{2}h_{\mu\nu,\alpha})\gamma_{(0)}^\mu\gamma_{(0)}^\nu. \quad (15)$$

However, $h_{\mu\alpha,\nu}P^\nu = dh_{\mu\alpha}/dt$ so that the first term in the integral is just a vanishing surface term. Thus only the second term survives and we are left with

$$\gamma_{\alpha(1)} = \frac{1}{2}\int_{-\infty}^{\infty} dt h_{\mu\nu,\alpha}\gamma_{(0)}^\mu\gamma_{(0)}^\nu. \quad (16)$$

We now require the metric produced by a string loop if we are to calculate the geodesic deflection; in the weak field limit, this problem has been solved. The configuration of a string loop is described by the position of the string $f^\mu(\sigma, t)$, where t is a time variable and σ is a parameter along the loop. The equations of motion for the string in Minkowski space are given by

$$\ddot{f}^\mu - f''^\mu = 0, \quad (17)$$

with the constraints

$$\dot{f}^\mu f'_\mu = 0, \quad \dot{f}^2 + f'^2 = 0. \quad (18)$$

Dots here refer to derivatives with respect to t while primes refer to derivatives with respect to σ . It is convenient to choose,

$$f^0 = t \quad (19)$$

and to write the string solutions as a superposition of traveling waves with non-linear constraints [13], namely,

$$\mathbf{f}(\sigma, t) = \frac{\mathbf{a}(\sigma - t) + \mathbf{b}(\sigma + t)}{2}, \quad (20)$$

$$\mathbf{a}'^2 = \mathbf{b}'^2 = 1. \quad (21)$$

For any closed loop of length L , solutions for \mathbf{f} must satisfy the periodic condition $\mathbf{f}(\sigma + L, t) = \mathbf{f}(\sigma, t)$. In the center of mass frame of the loop, the functions \mathbf{a} and \mathbf{b} are periodic as well, but this is not true in general. The description of the loop as given in eq. (20) also applies to loops that have a net momentum if we use the boundary condition $\mathbf{a}(\sigma - t) - \mathbf{a}(\sigma - t + L) = \mathbf{b}(\sigma + t + L) - \mathbf{b}(\sigma + t) = \mathbf{\Delta}$, where $\mathbf{\Delta}$ is the loop's center of mass velocity.

The energy-momentum tensor of the string is given in terms of f by

$$T^{\mu\nu} = \mu \int d\sigma (\dot{f}^\mu \dot{f}^\nu - \dot{f}'^\mu \dot{f}'^\nu) \delta^{(3)}(\mathbf{x} - \mathbf{f}(\sigma, t)). \quad (22)$$

With $T^{\mu\nu}$ one can write the solution to eq. (10) as an integral over a Greens function in retarded time, explicitly giving us

$$h_{\mu\nu}(\mathbf{x}, t) = 4G \int d^3x' \frac{S_{\mu\nu}(\mathbf{x}', \tau)}{|\mathbf{x} - \mathbf{x}'|}, \quad (23)$$

where $\tau = t - |\mathbf{x} - \mathbf{x}'|$ is the retarded time. Using the stress-energy defined in eq. (22), we can evaluate the spatial integral in eq. (23),

$$h_{\mu\nu}(\mathbf{x}, t) = 4G\mu \int d\sigma \frac{F_{\mu\nu}(\sigma, \tau)}{|\mathbf{x} - \mathbf{f}| - (\mathbf{x} - \mathbf{f}) \cdot \dot{\mathbf{f}}}, \quad (24)$$

where

$$F_{\mu\nu}(\sigma, t) = \dot{f}_\mu \dot{f}_\nu - \dot{f}'_\mu \dot{f}'_\nu - \eta_{\mu\nu} \dot{f}^2. \quad (25)$$

Let us use eq. (24) to test the validity the weak field approximation. Derivatives of f_μ are of order unity, so it follows we may treat $F_{\mu\nu}$ as order one. The integral over σ gives a term of order L , the loop length. Roughly then, the perturbation is small, *i.e.* $h_{\mu\nu} \ll 1$, when $|\mathbf{x} - \mathbf{f}| \gg G\mu L$. The string energy density is given by $G\mu \lesssim 10^{-6}$, so that the weak field approximation will break down only for photons which come within a small fraction of the loop length of striking the string itself, implying that, for most lensing scenarios, the approximation is valid. There is, however, an exception to this estimate in the case of cusps. Cusps are points on the loop which momentarily achieve the speed of light as the string oscillates, and, if the velocity of the cusp points in the direction of the photon trajectory, the deflection can be singular [14]. However, cusps only occur instantaneously, and the probability of a photon encountering one may be neglected.

Eq. (24) might seem to be the appropriate starting point for calculating ray deflections, but we shall see that it is more convenient to solve this problem in Fourier rather than coordinate space. To avoid confusion, let us use the following conventions,

$$F(x^\mu) = \frac{1}{(2\pi)^4} \int d^4k e^{-ik_\lambda x^\lambda} \tilde{F}(k^\mu),$$

$$\tilde{F}(k^\mu) = \int d^4x e^{ik_\lambda x^\lambda} F(x^\mu),$$

and consider eq. (10) again. Transformed, it becomes

$$-k^\lambda k_\lambda \tilde{h}_{\mu\nu} = -16\pi G \tilde{S}_{\mu\nu}. \quad (26)$$

Now we choose the unperturbed photon trajectory to be

$$\mathbf{x} = \hat{\gamma} t$$

and use $\tilde{h}_{\mu\nu,\alpha} = -ik_\alpha \tilde{h}_{\mu\nu}$, to write

$$I_\alpha \equiv \int dt h_{\mu\nu,\alpha}(t, \hat{\gamma}t) = -\frac{G}{\pi^3} \int dt \int d^4k e^{-itk_\lambda \gamma^\lambda} ik_\alpha \frac{\tilde{S}_{\mu\nu}}{k^\lambda k_\lambda}, \quad (27)$$

where all integrals are implicitly evaluated over an infinite range. The integral over time can be evaluated, and just transforms the exponential into a delta function $2\pi\delta(\hat{\gamma} \cdot \mathbf{k} - k_0)$. If we now decompose the wave vector \mathbf{k} into components parallel and perpendicular to $\hat{\gamma}$ so that $\mathbf{k} = (k_\parallel, \mathbf{k}_\perp)$, where $\mathbf{k} \cdot \hat{\gamma} = k_\parallel$ and \mathbf{k}_\perp is a two dimensional vector perpendicular to $\hat{\gamma}$ then the delta function becomes $\delta(k_\parallel - k_0)$, which allows us to evaluate the integral over k_0 . What remains is an integral over the three dimensional vector \mathbf{k}

$$I_\alpha = \frac{2G}{\pi^2} \int dk_\parallel d^2k_\perp \frac{ik_\alpha \tilde{S}_{\mu\nu}}{k_\perp^2}, \quad (28)$$

where k_\perp refers to the magnitude of \mathbf{k}_\perp . To make any more progress, we need to evaluate \tilde{S} in terms of \mathbf{f} . From eq. (22) one may infer that

$$\tilde{S}_{\mu\nu} = \mu \int d\sigma \int dt F_{\mu\nu}(\sigma, t) e^{ik_0 t} e^{-i\mathbf{k} \cdot \mathbf{f}(\sigma, t)}. \quad (29)$$

One should note that \mathbf{f} is measured from an origin chosen somewhere along the zeroth order photon trajectory and *not* from the loop center of mass. Later we shall find it more convenient to decompose \mathbf{f} into a component \mathbf{r} measured from the center of mass and \mathbf{x}_0 measured from the origin on the photon path, but for compactness we stay with \mathbf{f} for now. Replacing k_0 with k_\parallel , we can substitute eq. (29) into eq. (28) to get

$$I_\alpha = \frac{2G\mu}{\pi^2} \int d\sigma \int dt \int dk_\parallel d^2k_\perp \frac{ik_\alpha}{k_\perp^2} F_{\mu\nu} e^{ik_\parallel(t-f_\parallel)} e^{-i\mathbf{k}_\perp \cdot \mathbf{f}_\perp}, \quad (30)$$

where we have decomposed \mathbf{f} into its parallel and perpendicular components.

At this point it is necessary to choose α . If we want to know the redshift induced by the presence of a string, we would solve eq. (30) for $k_\alpha \rightarrow k_\parallel$; we will do this in the appendix to compare our results with previous work, but for now, we are interested in the deviation of the photon path from its zeroth order direction. Thus we consider the components $k_\alpha \rightarrow k_{\perp i}$. In this case, one may perform the integral over k_\parallel to produce a delta function $\delta(t - f_\parallel(\sigma, t))$, and so integrate out the time leaving

$$I_{\perp i} = \frac{4G\mu}{\pi} \int d\sigma \left[\frac{F_{\mu\nu}}{1 - \dot{f}_\parallel} \int d^2k_\perp e^{-i\mathbf{k}_\perp \cdot \mathbf{f}_\perp} \frac{ik_{\perp i}}{k_\perp^2} \right]_{t=t_0}, \quad (31)$$

where t_0 is the solution to

$$f_\parallel(t_0, \sigma) = t_0. \quad (32)$$

The integration over \mathbf{k}_\perp can be evaluated by recognizing that $e^{-i\mathbf{k}_\perp \cdot \mathbf{f}_\perp} / k_\perp^2$ is proportional to the Fourier transform of the Greens function for the two dimensional Laplacian operator, $-\pi \log(f_\perp^2)$. The final result is suprisingly simple,

$$I_{\perp i} = 8G\mu \int d\sigma \left[\frac{F_{\mu\nu}}{1 - \dot{f}_\parallel} \frac{f_{\perp i}}{f_\perp^2} \right]_{t=t_0}. \quad (33)$$

Finally, if we define the two dimensional vector $\bar{\alpha} = \hat{\gamma}_\perp(t \rightarrow -\infty) - \hat{\gamma}_\perp(t \rightarrow \infty)$ to be the deviation of the photon from its zeroth order trajectory, then from eq. (16) and eq. (33) we will get

$$\bar{\alpha} = -4G\mu \int d\sigma \left[\frac{F_{\mu\nu}(\sigma, t) \gamma^\mu \gamma^\nu \mathbf{f}_\perp}{1 - \dot{f}_\parallel} \frac{\mathbf{f}_\perp}{f_\perp^2} \right]_{t=t_0}, \quad (34)$$

where t_0 is determined by solving eq. (32).

IV. GRAVITATIONAL LENSING

A. Basic Lens Theory

In the previous section we derived an expression for the deflection of the photon momentum that passes near a cosmic string loop. Now we would like to use this expression to determine how an intervening string loop affects the images of various sources. Let us define an origin which is located at the center of mass of the loop, so the vector $\mathbf{r}(\sigma, \mathbf{t})$ will trace the loop measured from this origin. Further, we shall define a second vector \mathbf{x}_0 which points from the loop center of mass to the location of the photon at $t = 0$, so we may rewrite \mathbf{f} as the difference $\mathbf{r} - \mathbf{x}_0$. Now let us define the optical axis as the line connecting the loop center of mass to the observation point, that is \mathbf{r}_{\parallel} and \mathbf{x}_{\parallel} both point in the direction defined by the ray connecting the loop center of mass with the observer. Since the source rays which are likely to be affected by the loop come in at very shallow angles, we can treat them as rays parallel to the optical axis for the purposes of calculating α . We shall also assume that the deflection occurs instantaneously in the lens plane defined as the plane normal to the optical axis located at the loop center of mass. In each case, these approximations are accurate to terms of order the loop size over the distance of the source or observer to the lens (whichever is smaller). For the loops we shall be considering, these approximations will be more than adequate, since typical distances are on the order of the horizon while the loop size is about a factor $\Gamma G\mu$ smaller than that.

In Fig. 1 we show a schematic representation of the lensing system. A source lies in a plane perpendicular to the optical axis a distance D_{ls} from the lensing plane at the point S . The two dimensional vector in the source plane $\boldsymbol{\eta}$ points from the optical axis to the source. A ray emitted from the source intersects the lensing plane at I , and the two dimensional vector in the lensing plane $\boldsymbol{\xi}$ points from the optical axis to I . At I , the ray is deflected by the vector $\bar{\alpha}$. To be observed, the ray must intersect the observer O at a distance D_l from the lens plane on the optical axis. For small deflection angles, this condition is met if

$$\boldsymbol{\eta} = \frac{D_s}{D_l} \boldsymbol{\xi} - D_{ls} \bar{\alpha}(\boldsymbol{\xi}), \quad (35)$$

where D_s is the distance from the observer to the source plane. This formula, referred to as the lens equation, gives us the location of a source, $\boldsymbol{\eta}$, given the location of its image, $\boldsymbol{\xi}$. Usually we are interested in the inverse problem, namely given a source location, where are its images located. Note that the inverse of eq. (35) is not necessarily single valued, so it is possible that a particular source has multiple images.

We must digress for a moment to discuss exactly what is meant by distance in the lens equation, for in an expanding universe, several definitions of distance are possible. For example, if the universe were seeded with sources of a known absolute luminosity, one could define the distance to any of these sources to be proportional to the square root of the absolute luminosity divided by the observed flux. However, for the case of gravitational lenses (Fig. 1), we are interested in the angular size of an image as it appears to a terrestrial observer, and we find that the luminosity distance is not the best choice. We should then like to define the angular diameter distance, d_A , as the ratio of the object size and the angle that the object subtends at the location of the observer. Then, using an FRW metric and assuming a flat, matter dominated universe with no cosmological constant, it is easy to show that the angular diameter distance is [12]

$$d_A(z_1, z_2) = \frac{2}{H_0(1+z_2)} \left[\frac{1}{\sqrt{1+z_1}} - \frac{1}{\sqrt{1+z_2}} \right]. \quad (36)$$

The lengths D_s , D_l and D_{ls} are all angular diameter distances given by this equation².

Given an extended source, not only can a lens change the location and number of images observed, it can also affect the magnification and shape as well. To see this, let us, for the sake of convenience, first redefine the lens equation in terms of dimensionless variables. The loop length L is defined in terms of the energy of the loop as E/μ . A convenient length scale for us is the loop radius which we define as $R \equiv L/2\pi$. If we define

$$\mathbf{x} = \frac{\boldsymbol{\xi}}{R} \quad (37)$$

²A word of caution: the real universe, especially at late times, is clumped and only homogeneous on average. A better distance choice may come from models like the Dyer–Roeder equation [15], but for the present we prefer not to consider these technical questions.

$$\mathbf{y} = \frac{\eta D_l}{D_s R} \quad (38)$$

$$\boldsymbol{\alpha}(\mathbf{x}) = \bar{\boldsymbol{\alpha}}(\boldsymbol{\xi}) \frac{D_{ls} D_l}{D_s R}, \quad (39)$$

then the lens equation is reduced to

$$\mathbf{y} = \mathbf{x} - \boldsymbol{\alpha}(\mathbf{x}). \quad (40)$$

One interesting question to ask, then, is given a narrow pencil beam emitted by the source which subtends a solid angle $d\omega^*$, what is the solid angle $d\omega$ subtended by its image? This question is directly related to the issue of magnification as the observed flux relative to the emitted flux is just the ratio of the solid angles $d\omega/d\omega^*$. The answer may be found by looking at the Jacobian matrix

$$A_{ij} = \frac{\partial y_i}{\partial x_j}, \quad (41)$$

which gives us the magnification factor

$$\mu(\mathbf{x}) = \frac{1}{\det A(\mathbf{x})}, \quad (42)$$

and the magnification is defined as the absolute value, $|\mu|$. For many lensing systems, there will exist curves in \mathbf{x} for which $\mu(\mathbf{x})$ is infinite or equivalently the determinant of the Jacobian vanishes. These curves are referred to as critical curves, and the corresponding map of the critical curves into the source plane are called caustics. Caustics play an important role in determining the number of possible images. Consider a system for which the Jacobian never vanishes. The lens equation is then globally invertible and therefore single valued. Thus when there are no caustics, there can be only one image of the source. If there exists a caustic, then the lens equation is only locally invertible and there may be multiple images. In fact there are many general theorems which can be proved about caustics and images; we shall not discuss them here, but the interested reader is directed to a detailed review of the subject of gravitational lensing by Schneider, Ehlers and Falco [16].

We have seen how a lens can affect the magnification of an image, and we would now like to show how a lens can change the shape of the observed image. We shall restrict ourselves here to a discussion of small sources so that we may treat the problem differentially. Consider two points on a source separated by a distance \mathbf{Y} . From the lens equation we can see, to first order in the Taylor expansion, that the image displacement \mathbf{X} will be

$$\mathbf{X} = A^{-1} \mathbf{Y}. \quad (43)$$

Now consider a source that is a small circle. From eq. (43) we can surmise that the image will be an ellipse with major and minor axis pointing along the eigenvectors of A^{-1} with lengths equal to their eigenvalues. The most dramatic results will appear near a critical curve. Here, usually one of the eigenvalues of A^{-1} blows up, so that images are not only magnified, but stretched as well. What is observed is a stretched image, but since the flux grows in proportion to the area, one observes an image which appears to be a stretched version of the source but with the original brightness.

B. An Analytic Example: The Perpendicular Circular Loop

In this subsection, we will consider a simple example of a circular loop which lies in a plane perpendicular to the optical axis. This problem has the virtue of being analytically soluble, and it will also illustrate some of the features that might be expected for a more general loop. Most notably, there is a discontinuity in the deflection $\boldsymbol{\alpha}$ as light rays go from passing through the loop to passing outside it which noticeably influences the resulting images.

Let us begin by choosing the z direction to point along the optical axis. For the perpendicular circular loop, the configuration of the string is given by

$$\mathbf{r} = R \cos\left(\frac{t}{R}\right) \left[\cos\left(\frac{\sigma}{R}\right), \sin\left(\frac{\sigma}{R}\right), 0 \right], \quad (44)$$

where R is the maximal radius of the loop. From eq. (25), one can see that for any planar loop perpendicular to the optical axis, $\gamma^\mu \gamma^\nu F_{\mu\nu} = 1$. Also, there is no parallel component in \mathbf{r} , so $\dot{f}_\parallel = 0$. Thus, using eq. (34) and eq. (37), we can write the deflection as

$$\alpha(\mathbf{x}) = -4G\mu \frac{D_{ls}D_l}{RD_s} \int_0^{2\pi} d\theta \frac{\mathbf{x} - \mathbf{r}'(t_0)}{x^2 + r'^2(t_0) - 2xr' \cos \theta}, \quad (45)$$

where $\mathbf{r}' = \mathbf{r}(\mathbf{t}_0)/R$, $x \equiv |\mathbf{x}|$ and t_0 , defined by eq. (32), is a constant. The behavior of this integral is most easily seen by analytical continuation on to the complex plane. If we change variables to $z = \rho e^{i\theta}$, then the integral in eq. (45) is a contour integral along the $\rho = 1$ circle in the complex plane and hence reduces to a sum of complex residues. One finds that for image points such that $x < r'$, the residues cancel and there is no deflection, but for image points such that $x > r'$, the result is non-zero³. We point this out because in principle the deflection for any loop can be reduced to finding residues of a complex contour integral. In practice, however, the problem is complicated by the need to solve eq. (32) to get t_0 as a function of σ , and there appears to be no advantage in using the calculus of residues over numerical integration to find α , although there may be other cases aside from the circular loop where this method could be usefully applied. Returning to the circular loop, one finds that $\alpha(\mathbf{x}) = 0$ if $|\mathbf{x}| < r'$ and

$$\alpha(\mathbf{x}) = -8\pi G\mu \frac{D_{ls}D_l}{RD_s} \frac{\mathbf{x}}{x^2}, \quad \text{if } |\mathbf{x}| > r'.$$

For rays passing outside the loop, the deflection is exactly the same as if the loop were replaced by a point mass. Inside the loop, the ray is undeflected, a feature which distinguishes a normal circular loop from a point source.

Given the deflection, we will now consider the magnification, specifically looking for the caustics. The Jacobian matrix can be written as $A_{ij} = \delta_{ij} - \alpha_{i,j}$, so for the circular loop we find that when $x > r'$,

$$A = \begin{bmatrix} 1 - C(x_2^2 - x_1^2)/x^4 & -2Cx_1x_2/x^4 \\ -2Cx_1x_2/x^4 & 1 - C(x_1^2 - x_2^2)/x^4 \end{bmatrix}$$

where $C = 8\pi G\mu D_{ls}D_l/RD_s$ and \mathbf{x} is given by its components (x_1, x_2) . For $x < r'$, A is just the identity matrix and $\det(A) = 1$. For $x > r'$, the determinant of A is given by

$$\det(A) = 1 - \frac{C^2}{x^4}. \quad (46)$$

One real root, namely $x = \sqrt{C}$, is proportional to the Einstein radius $R_e = R\sqrt{C}$. Note that this definition is consistent with the familiar definition of the Einstein radius of a point mass, namely $R_e = \sqrt{4GM D_{ls}D_l/D_s}$, where for a string the mass is just $M = 2\pi R\mu$. So, if $\sqrt{C} > r'$, the loop lens will have a circular critical curve with radius \sqrt{C} , but if $\sqrt{C} < r'$ there will be no critical curve. In the latter case, the loop would be difficult to detect because there will be only one image of the source which will not be significantly distorted or magnified. In the former case ($\sqrt{C} > r'$) there are, strictly speaking, two critical curves because the discontinuity at the location of the string should be smoothed out on a scale given by the thickness of the string. Then the first critical curve is the usual Einstein ring with radius \sqrt{C} and the second occurs because the determinant of A must change from a positive value (namely 1) inside the loop to a negative value just outside the loop (namely $1 - C^2/r'^4$) and hence $\det A = 0$ when the light ray passes through the string⁴. For the case of the circular loop, we can analytically invert the lens equation as well, and after a little algebra we find

$$x_1 = \frac{y_1}{2} \left(1 \pm \sqrt{1 + \frac{4C}{y^2}} \right) \quad (47)$$

$$x_2 = \frac{y_2}{2} \left(1 \pm \sqrt{1 + \frac{4C}{y^2}} \right) \quad (48)$$

when $x > r'$, but $\mathbf{x} = \mathbf{y}$ when $x < r'$. To help visualize this rather complicated picture, we show in Fig. 2 a series of images for a circular source as it is displaced further away from the optical axis. We have chosen a loop radius $r' = 1$ with a value of $C = 2.25$ corresponding to an Einstein radius of 1.5. It follows that there are two critical curves with radii $r_c = 1$ and 1.5

³This discontinuous behavior will hold for all loops and is easily understood in terms of the motion of poles in the complex plane.

⁴This second critical curve is of no observable interest since the string thickness is a mere 10^{-30} cms or so. It does have formal significance when considering lensing theorems. In the following section, where we give image maps, we shall ignore the effects of light rays that actually pass through the string.

C. Numerical Examples

The perpendicular circular loop is one of the few cases which may be treated analytically, but it is not a very generic loop. In this subsection, we would like to consider a few examples which represent more general cases of cosmic string lenses. We will consider loops which are neither planar nor oriented in any special way with respect to the optical axis and are characterized by reasonable astrophysical parameters.

Suppose that we have a bright galaxy or cluster of galaxies at a redshift of $z \sim 2$ which is lensed by a cosmic string loop. Will a “typical” loop produce any observationally distinctive images? The answer to this question depends roughly on the value of the Einstein radius of the system. For a general loop, we define the Einstein radius as

$$R_e \equiv \sqrt{8\pi G\mu R \frac{D_{ls}D_l}{D_s}}, \quad (49)$$

so if we were to replace the loop with a point source with mass equal to the mass of the loop, the critical curve would be a circle with the Einstein radius. If $R_e \gg R$ then the images which would be significantly distorted by the string loop will appear to be similar to those of an equivalent point source. If $R_e \ll R$, then the loop will not have a significant affect on any images of the source as most of the mass of the loop will lie outside the Einstein radius. If string loops are to produce distinctive images, we should have $R_e \sim R$. So let us consider what may be reasonable parameters for a loop lens system.

We can estimate the size of a “typical” string loop on the basis of the string network evolution described in Sec. II. Loops are expected to be produced from the network of long strings with typical size $R \sim \Gamma G\mu t(z=1)/2\pi$. These loops gradually lose their energy to gravitational radiation (eq. (1)) but survive for about one Hubble period. (We are assuming that the loops are not further fragmented significantly by self-intersections. If that is the case, we would need to divide the size estimate by the expected number of fragmentations and factor in the survival period in the estimate of the lensing probability in Sec. II.) Then, using this value for the loop radius, taking $\Gamma = 60$ and locating a source at $z = 2$ and the loop at $z = 1$, the Einstein radius is given by

$$R_e = R \sqrt{\frac{16\pi^2 D_{ls}D_l}{\Gamma t D_s}} \sim R \quad (50)$$

— which is in just the right range for distinctive string lenses. Further note that the result $R_e \sim R$ is independent of the string tension μ and so the stringy nature of loop lensing is important for strings of any mass density. We therefore expect that the images produced by string loops will have characteristic features of stringy lenses, thus offering the realistic hope that strings may be observed definitively through gravitational lensing⁵.

We shall consider two classes of loops to illustrate the kinds of images that one may observe with cosmic string loops. The first is a mixture of the fundamental and the first excited mode

$$\mathbf{r} = \frac{R}{2} \left\{ \sin \sigma_- \mathbf{i} + \frac{1}{2} \sin 2\sigma_+ \mathbf{j} + \left[\cos \sigma_- + \frac{1}{2} \cos 2\sigma_+ \right] \mathbf{k} \right\}, \quad (51)$$

where $\sigma_- = (\sigma - t)/R$ and $\sigma_+ = (\sigma + t)/R$. We will call this the “two-loop” for short since it is a superposition of a fundamental mode with a frequency two mode. The second loop configuration is a class of loops found by Turok [17] which is the general solution for a loop with frequency one and three Fourier modes. This solution has the form

$$\begin{aligned} \mathbf{r} = \frac{R}{2} \left\{ \left[(1 - \alpha) \sin \sigma_- + \frac{1}{3} \alpha \sin 3\sigma_- + \sin \sigma_+ \right] \mathbf{i} \right. \\ \left. - \left[(1 - \alpha) \cos \sigma_- + \frac{1}{3} \alpha \cos 3\sigma_- + \cos \phi \cos \sigma_+ \right] \mathbf{j} \right. \\ \left. - \left[2\sqrt{\alpha(1 - \alpha)} \cos \sigma_- + \sin \phi \cos \sigma_+ \right] \mathbf{k} \right\}. \end{aligned} \quad (52)$$

We shall call this the “three-loop” for short. In general, the coordinate system which defines $\{\mathbf{i}, \mathbf{j}, \mathbf{k}\}$, *i.e.* the loop coordinates, can be rotated with respect to the optical axis, which, for convenience, we shall define to be the z axis.

⁵The wiggles on long strings can probably also be regarded as loops of size R and hence the lensing by long strings would mimic that of a linear array of loops. This would be another characteristic feature of lensing by cosmic strings.

The relative orientation of the systems can be described by the three Euler angles. However, we are not particularly interested in the orientation in the sky, so it is sufficient to consider only two of the three. Thus, if we start with the systems $\{\mathbf{x}, \mathbf{y}, \mathbf{z}\}$ and $\{\mathbf{i}, \mathbf{j}, \mathbf{k}\}$ aligned, we shall first rotate the loop in the $x - y$ plane from x to y through an angle θ_1 . Then we shall tilt the loop with respect to the observer by rotating in the $y - z$ plane from y to z through an angle θ_2 , giving us the final orientation of the loop coordinates with respect to the optical coordinates.

To find the images for a given source is a numerically non-trivial problem because one has to invert eq. (35) to get ξ as a function of η . This involves finding simultaneous roots of two equations in two dimensions. But, as there are no general methods to solve such a problem, we are left with no choice but to map the entire image plane (ξ) into the source plane (η) and then consider the inverse mapping. (In practice, a lattice of points in the image plane is mapped on to the source plane.) To locate the images for a particular source point, we test every triangle in the image plane that can be formed by three neighboring points on the lattice. If, when mapped to the source plane, the image triangle encompasses a source point, then we know that the source has an image located somewhere inside the image triangle. Calculating α entails performing one numerical integration, so the inversion process is reasonably cheap with regards to cpu time and good resolution is possible. The triangle search method, however, has one failing when finding images with strings. Since α will be discontinuous for light rays which pass just to either side of the string, image triangles which are formed by points on either side of the loop may encompass sources which they would not if all the image points were on one side or the other of the loop. These are spurious images as they require the light rays to pass through the string itself, so we have rejected these points when constructing the images of specific sources (see the discussion in Sec. IV B).

Let us now use this technology to generate some images for the loops which we have discussed in this section⁶. In Fig. 3 we consider the two-loop aligned with the optical coordinates so $\theta_1 = 0$ and $\theta_2 = 90$. The phase of the loop is given by ψ which is defined as the time at which the light ray intersects the lens plane — the plane normal to $\hat{\gamma}$ and containing the loop's center of mass. For this first example, $\psi = 0$. The source is located at a redshift of two, the loop at a redshift of one and the loop radius has been chosen to give an Einstein radius of $R_e/R = 1$ which we have shown to be a typical value. This choice corresponds to a loop radius of $R = 2.3 \times 10^{-5} H_0^{-1}$. The upper left window shows the mapping onto the source plane of a series of vertical lines spaced evenly at intervals of $0.02 R$ in the image plane. The upper right panel shows the critical curves, the images of infinite magnification, for this example. The lower left panel shows the unlensed images of a grid of source circles each defined by 15 points. Finally, the lower right panel shows the images observed for the loop lens along with the projection of the loop. (This field of sources is primarily illustrative; realistic galaxies are larger compared to realistic loops, and a subsequent set of figures will address this issue.) Images were found by the aforementioned method with a grid resolution of 200×200 . Figure 4 shows the same two-loop now rotated through $\theta_2 = 0$, but now we only show the lensed field and the critical curves. Figure 5 shows the same information as Fig. 4 but for a three-loop instead. The loop parameters in this case were chosen to match those used by Stebbins [9]: $\alpha = 0.5$, $\sin \phi = 0.5$, $\theta_1 = \theta_2 = 50$ and $\psi = 0$. Finally, Fig. 6 shows the same three-loop, but now at a phase $\psi = 120$.

In the next series of figures, we consider more realistic images that might be observed with a loop lens and a distant galaxy. Recall that we expect the typical loop radius to be $\Gamma G\mu t/2\pi$. Taking $\Gamma = 60$ and locating the loop at a redshift of $z = 1$, one finds that the loop subtends an angle of $3.2 G\mu_6$ arc sec, where $G\mu_6 \equiv 10^6 G\mu$. We have already stated that $G\mu_6 \sim 1$ if strings are responsible for seeding structure formation, but we can more precisely constrain this value. The best data comes from the observation of the cosmic microwave background. If strings are responsible for the large scale temperature fluctuations observed by COBE, then $G\mu_6 = 1.5 \pm .5$, as calculated by Bennett, Stebbins and Bouchet [2]. Below this range, strings cease to be interesting candidates for structure formation. Upper limits on the string tension have also been set by observing millisecond pulsars. The most recent data suggests that $G\mu_6 < 2$ [3]. We consider $G\mu_6 = 1.25$ so that our loop diameter subtends an angle of 4 arc seconds. The angle subtended by the visible portion of a distant galaxy at redshift $z \sim 2$, is roughly 1 arc second. In Figs. 8-10, we show several examples of the images formed with a circular source with radius 1 arc sec for each of our loop examples with $R = 2$ arc sec. In each case the Einstein radius was fixed to be one corresponding to a source redshift of about two. Source locations were chosen in these examples primarily to show some of the more interesting features of the loop lenses.

⁶We will not explicitly consider loops that have a net velocity though our formalism applies directly to this case. We expect that the lensing by moving loops will look very similar to the lensing by stationary loops but that the loop will have a different effective shape due to the condition in eq. (32).

V. DISCUSSION

The examples in the previous section may not represent an exhaustive sample of possible loop configurations, but they do show some of the generic features of loop lenses. For both the two-loop and the three-loop, we have considered configurations for which the projected loop lies near the Einstein radius and more compact configurations which reside well inside the Einstein radius. For the former case, Figs. 3, 5, 7 and 9, we notice that, like the perpendicular circular lens, we can have images which pass through the center of the loop and lie close to where the unlensed image would be. This is perhaps the distinguishing feature of loop lens images. In Figs. 7 and 9 we see examples of relatively undistorted images encircled by arcs and rings in a manner unlike what one would expect for a more homogeneous lens mass distribution. The more compact loops produce, unsurprisingly, less spectacular images. In Fig. 10 there are some examples with three images which may be distinguishable from ordinary lenses. Still, for all loops, one feature always differentiates them from ordinary lenses: namely that the lens itself is dark.

Would the observation of lensed images lacking an observed lens in itself confirm the existence of cosmic string loops? Unfortunately, the answer is no; the existence of dark lenses in and of itself would not be conclusive since there are other possibilities. For example, it has been suggested that dark matter could form halos without a luminous component and these would result in dark lenses [18,19]. Kandaswamy, Rees and Chitre [19] found that a single dark matter halo is not sufficiently dense to produce multiple imaging, but the alignment of two such halos could. Typical image separation was on the order of a few arc seconds, similar to the string loop case. However, these halos will have a distribution of matter consistent with collisionless particles (*i.e.* an isothermal sphere), so their images should be distinguishable from string loops. A second possibility is that the net effect of many distant lenses which individually would not produce multiple images could add together to produce such an effect. This, however, has been shown to be statistically unlikely [20]. Perhaps the simplest explanation for a dark lens is that it is not dark at all. A cluster of galaxies could produce two images which are separated on arc second scales, with a third located typically an arc minute away. The third image could easily go unnoticed creating the false impression of a dark lens [21]. But again, the images should be distinctly different than those of a string loop. The good news then is that string loop lenses are distinguishable from other dark lens possibilities, especially loops which are not compact with respect to their Einstein radius. Should a dark lens be confirmed, detailed observations of the image structure ought to determine the nature of the lens.

Another possibility that we have not examined in detail in this paper but that is amenable to an identical analysis is the lensing due to wiggly long strings. The presence of wiggles on long strings means that the long string can probably be regarded as a sequence of small loops. In this case, we should observe a linear sequence of dark lenses with each lens having the characteristics of a string loop lens. Such a lens is unlikely to occur in the context of any other model.

VI. CONCLUSION

In this paper we have derived a method for calculating the deflection of light rays due to the gravitational field of an oscillating string loop. We have shown that this problem can be reduced to an effective static problem, greatly simplifying calculations. The formalism was then applied to the problem of gravitational lensing by cosmic strings, and using typical loop parameters, we have shown that a loop lens produces images on arc second scales, similar to galactic size objects. Specifically, we find that for $G\mu \sim (1 - 2) 10^{-6}$ — values consistent with structure formation, microwave background anisotropies and millisecond pulsar timing limits — strings can produce images separated on arc second scales which would be observable by both ground based telescopes and the Hubble space telescope and would have features that are distinctly different from other dark lens candidates. This suggests that string loops can be definitively observed as gravitational lenses. Furthermore, the lensing due to long strings would appear like a linear sequence of lensings due to loops and these would be the unmistakable fingerprints of cosmic strings.

-
- [1] A. Vilenkin and E. P. S. Shellard, *Cosmic Strings and other Topological Defects* (Cambridge University Press, Cambridge, 1994)
 - [2] D. P. Bennett, A. Stebbins and F. R. Bouchet, *Astrophys J.* **399**, L5 (1992)
 - [3] R.R. Caldwell and B. Allen, *Phys. Rev.* **D45**, 3447 (1992).
 - [4] A. Vilenkin, *Ap. J.* **L51**, 282 (1984); *Nature* **322**, 613 (1986).

- [5] C.J. Hogan and R. Narayan, M.N.R.A.S. **211**, 575 (1984).
- [6] J.R. Gott, Ap. J. **288**, 422 (1985).
- [7] B. Paczynski, Nature **319**, 567 (1986).
- [8] M. Hindmarsh in *The Formation and Evolution of Cosmic Strings*, eds. G.W. Gibbons, S.W. Hawking and T. Vachaspati, Cambridge University Press (1990).
- [9] A. Stebbins, Astrophys. J. **327**, 584 (1988)
- [10] D. P. Bennett and F. R. Bouchet, Phys. Rev. D **41**, 2408, 1990
- [11] B. Allen and E. P. S. Shellard, Phys. Rev. Lett. **64**, 119, 1990
- [12] P.J.E. Peebles, *Principles of Physical Cosmology*, Princeton University Press (1993).
- [13] T. W. B. Kibble and N. Turok, Phys. Lett **116B**, 141 (1982)
- [14] T. Vachaspati, Phys. Rev. D **35**, 1767 (1987)
- [15] C. C. Dyer and R. C. Roeder, Astrophys. J. **180**, L31 (1973)
- [16] P. Schneider, J. Ehlers and E. E. Falco, *Gravitational Lenses* (Springer-Verlag, New York, 1992)
- [17] N. Turok, Nuclear Physics **B242**, 520 (1984)
- [18] G. Hinshaw and L.M. Krauss, Ap. J. **320**, 468 (1987).
- [19] S. Kandaswamy, M. J. Rees and S. M. Chitre, Mon. Not. R. Astr. Soc. **224**, 283 (1987)
- [20] *ibid* pp. 461-466
- [21] R. Narayan, R. Blandford and R. Nityananda, Nature **310**, 112 (1984)

APPENDIX A: EFFECT OF A STRING LOOP ON THE ENERGY OF A PHOTON

The temperature fluctuations induced by cosmic string loops has previously been investigated by Stebbins [9], using the harmonic gauge as we have done here. Stebbins, however, used the real space retarded Greens function to find the change in γ_0 , but, as we are solving the problem in Fourier space, it is useful to compare our results. Let us return then to eq. (30) and replace k_α with k_\parallel or equivalently k_0 . If we rewrite the product $ik_\parallel e^{k_\parallel(t-f_\parallel)}$ as $1/(1-f_\parallel)d/dt(e^{k_\parallel(t-f_\parallel)})$, we can again evaluate the k_\parallel integral which now gives us

$$I_0 = \frac{4G\mu}{\pi} \int d\sigma \int dt \int d^2k_\perp \frac{F_{\mu\nu}}{(1-f_\parallel)} \frac{e^{-i\mathbf{k}_\perp \cdot \mathbf{f}_\perp}}{k_\perp^2} \frac{\partial}{\partial t} \delta(t-f_\parallel). \quad (\text{A1})$$

The time integral can be evaluated by parts leaving

$$\frac{4G\mu}{\pi} \int d\sigma \int d^2k_\perp \left[\frac{\partial}{\partial t} \left(\frac{F_{\mu\nu}}{(1-f_\parallel)} \frac{e^{-i\mathbf{k}_\perp \cdot \mathbf{f}_\perp}}{k_\perp^2} \right) \frac{1}{(1-f_\parallel)} \right]_{t=t_0}, \quad (\text{A2})$$

and we can again evaluate the \mathbf{k}_\perp integral as before. Finally, the temperature change caused by the loop is given by

$$\frac{\Delta T}{T} = -4G\mu \int d\sigma \gamma^\mu \gamma^\nu \left[\frac{\partial}{\partial t} \left(\frac{F_{\mu\nu}}{(1-f_\parallel)} \right) \frac{\log(f_\perp^2)}{(1-f_\parallel)} + \frac{2F_{\mu\nu}}{(1-f_\parallel)^2} \frac{\dot{\mathbf{f}}_\perp \cdot \mathbf{f}_\perp}{f_\perp^2} \right]_{t=t_0}. \quad (\text{A3})$$

The appearance of the logarithm in the first term in the above expression may be cause for concern as it appears to diverge for rays passing far from the loop. However, Stebbins [9] has proven, using conservation of energy that

$$\int d\sigma \gamma^\mu \gamma^\nu \left[\frac{\partial}{\partial t} \left(\frac{F_{\mu\nu}}{(1-f_\parallel)} \right) \frac{1}{(1-f_\parallel)} \right]_{t=t_0} = 0, \quad (\text{A4})$$

For rays far from the loop, *i.e.* $\mathbf{x}_0 \gg \mathbf{r}$, the logrithm can be expanded to leading order, $\log(f_\perp^2) \approx \log(x_0^2) - 2\mathbf{x}_0 \cdot \mathbf{r}/x_0^2$, which falls like the inverse of the distance and does not diverge.

For completeness, we sketch the proof of eq. (A4). Conservation of energy requires that $\partial^\nu T_{\mu\nu} = 0$, so we can certainly write

$$\int d^3x \int dt \delta(\mathbf{x} \cdot \hat{\gamma} - t) \partial^\nu T_{\mu\nu}(\mathbf{x}, t) = 0. \quad (\text{A5})$$

We are in essence performing the integral over the time slice as it appears in eq. (A1). Integrating the spatial components by parts, one can easily verify that eq. (A5) is equivalent to

$$\int d^3x \int dt \delta(\mathbf{x} \cdot \hat{\gamma} - t) \gamma^\nu \frac{\partial}{\partial t} T_{\mu\nu}(\mathbf{x}, t) = 0, \quad (\text{A6})$$

given that $t = \hat{\gamma} \cdot \mathbf{x}$ is implied by the delta function. Using eq. (22) as a guide, we can write the stress energy as

$$T_{\mu\nu} = \mu \int d\sigma \mathcal{T}_{\mu\nu}(\sigma, t) \delta(\mathbf{x} - \mathbf{f}(\sigma, t)), \quad (\text{A7})$$

and substituting into eq. (A6) gives us

$$\mu \int d\sigma \int d^3x \int dt \int dt' \delta(\mathbf{x} \cdot \hat{\gamma} - t) \gamma^\nu \frac{\partial}{\partial t} [\mathcal{T}_{\mu\nu}(\sigma, t') \delta(\mathbf{x} - \mathbf{f}(\sigma, t')) \delta(t - t')] = 0. \quad (\text{A8})$$

We have added the extra delta function to enable us to see how to evaluate this integral. Let us replace it with a Fourier integral and evaluate the derivative,

$$\mu \int d\sigma \int d^3x \int dt \int dt' \int dk \delta(\mathbf{x} \cdot \hat{\gamma} - t) \gamma^\nu \mathcal{T}_{\mu\nu}(\sigma, t') \delta(\mathbf{x} - \mathbf{f}(\sigma, t')) \frac{ik}{2\pi} e^{ik(t'-t)} = 0. \quad (\text{A9})$$

Now we can evaluate the integrals over t and \mathbf{x} , leaving us with

$$\mu \int d\sigma \int dt' \int dk \gamma^\nu \mathcal{T}_{\mu\nu}(\sigma, t') \frac{ik}{2\pi} e^{ik(t' - f_{\parallel}(\sigma, t'))} = 0, \quad (\text{A10})$$

which is equivalent to (rewrite the product of k and the exponential as a time derivative)

$$\mu \int d\sigma \int dt' \int dk \gamma^\nu \frac{\mathcal{T}_{\mu\nu}}{1 - \dot{f}_{\parallel}(\sigma, t')} \frac{\partial}{\partial t'} \delta(ik(t' - f_{\parallel}(\sigma, t'))) = 0. \quad (\text{A11})$$

This can be integrated by parts, finally giving us

$$\mu \int d\sigma \gamma^\nu \left[\frac{\partial}{\partial t} \left(\frac{\mathcal{T}_{\mu\nu}}{1 - \dot{f}_{\parallel}(\sigma, t)} \right) \frac{1}{1 - \dot{f}_{\parallel}(\sigma, t)} \right]_{t=t_0} = 0, \quad (\text{A12})$$

where t_0 is again the solution to $f_{\parallel}(\sigma, t_0) = t_0$. To recover eq. (A4), one may contract the above with γ^μ and recognize that $\gamma^\mu \gamma^\nu \mathcal{T}_{\mu\nu} = \gamma^\mu \gamma^\nu F_{\mu\nu}$.

We should point out that both terms in eq. (A3) are necessary for calculating the microwave background anisotropies produced by string loops. In examples, however, we found that the contribution of the logarithmic term to the temperature fluctuation was only a few percent at most, and so we suspect that, in general, the logarithmic term that was overlooked in Ref. [9] will not make a significant difference to the existing analyses [2].

FIG. 1. A schematic representation of a gravitational lensing system. The vectors η , ξ need not be coplanar. The vector $\bar{\alpha}$ is defined as the difference of unit vectors along SI and IO .

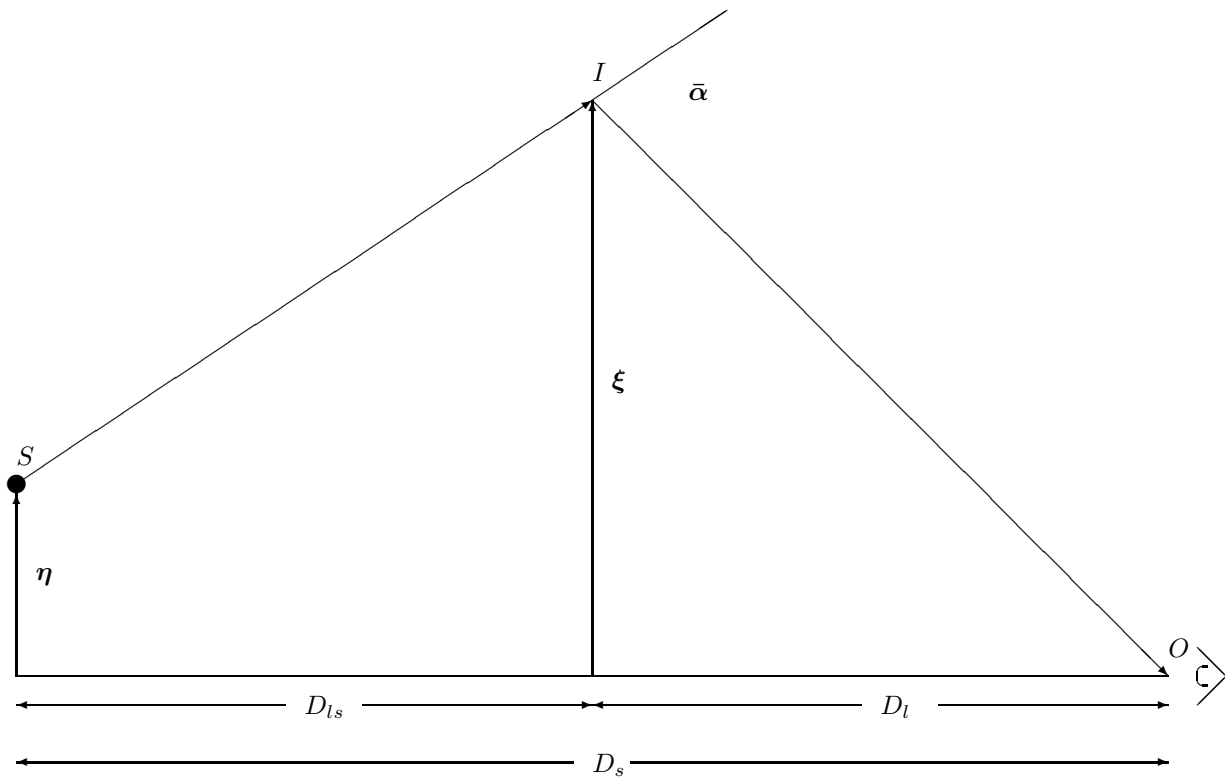


FIG. 2. The images resulting from a planar circular loop of radius one (solid circle) for a series of circular sources which spiral out from the origin. Hatching indicates images resulting from a particular source. The dashed line shows the Einstein radius selected for this example.

FIG. 3. Lensing by a two-loop rotated through $\theta_1 = 0$, $\theta_2 = 90$ and with phase $\psi = 0$. Each panel has dimensions $4R \times 4R$ where R is the size of the loop. The upper left panel shows the mapping of a grid of lines in the image plane onto the source plane. The upper right panel shows the critical curves in the image plane, *i.e.* the image points of infinite magnification. The lower left panel shows the unlensed images of a grid of circles each defined by 15 points. Finally, the lower right panel shows the lensed images along with the projection of the loop at time t_0 .

FIG. 4. The left panel shows the projected loop and images of a field of sources like those used in figure 3, but with a two-loop rotated through $\theta_1 = \theta_2 = 0$ and phase $\psi = 0$. The right panel shows the critical curve

FIG. 5. Same as figure 4, but with a three-loop rotated through $\theta_1 = \theta_2 = 50$ and phase $\psi = 0$

FIG. 6. Same as figure 4, but with a three-loop rotated through $\theta_1 = \theta_2 = 50$ and phase $\psi = 120$

FIG. 7. The upper left panel shows the caustic of a two-loop rotated through $\theta_1 = 0$, $\theta_2 = 90$ and phase $\psi = 0$. The other panels show the images as crossed points produced by a circular source whose unlensed image is given by the filled points. Also shown is the caustic.

FIG. 8. Same as figure 7 but with two-loop lens rotated through $\theta_1 = \theta_2 = 0$ and phase $\psi = 0$.

FIG. 9. Same as figure 7 but with a three-loop rotated through $\theta_1 = \theta_2 = 50$ and phase $\psi = 0$.

FIG. 10. Same as figure 7 but with a three-loop rotated through $\theta_1 = \theta_2 = 50$ and phase $\psi = 120$.

